

A POST-VOYAGER VIEW OF SATURN'S ENVIRONMENT

Some of the important results obtained in the magnetosphere of the planet Saturn by the two Voyager spacecraft and by Pioneer 11 are discussed. These include the absence of a significant tilt between the rotational and magnetic axes of the planet, and the discovery of a torus of very hot (about 6×10^8 K) dilute plasma associated with the orbits of the satellites Rhea and Dione.

INTRODUCTION

The environment of Saturn has been investigated by three spacecraft in the course of two years, beginning with the encounter of Pioneer 11 in September 1979, and followed by Voyager 1 and Voyager 2 in November 1980 and August 1981, respectively. "Environment," as used in this paper, may be defined as that part of the space surrounding the planet that is controlled by the planet's own magnetic field, i.e., its magnetosphere.* This definition excludes the planet itself and its atmosphere, the rings, and the satellites, but it includes energetic particles (consisting of ions and electrons), neutral particles, plasmas, and wave fields that may be present within the magnetospheric cavity, and the interaction of these particles and plasmas with the satellites and the rings. Even though the subject of this paper does not specifically include the satellites and the rings, a proper discussion and understanding of the planet's environment cannot be given without some knowledge of the solid bodies and of the particulate matter that populate the magnetosphere.

Figure 1 is a schematic view of most of the Saturnian system, showing the major inner satellites and the rings. The Saturnian system, outside of Saturn itself, is dominated by Titan, the largest Saturnian satellite and the only satellite in the solar system with an atmosphere. Outside Titan is located the small satellite Hyperion, while inside we see in sequence the satellites Rhea, Dione, Tethys, Enceladus, and Mimas. The interaction of these satellites with the magnetospheric plasma, energetic particles, plasma waves, and radio emissions has been found to be quite varied and complex.

Inward of Mimas the visible rings have a profound influence on energetic particles, as observed originally by the Pioneer investigators.¹ The Voyager instru-

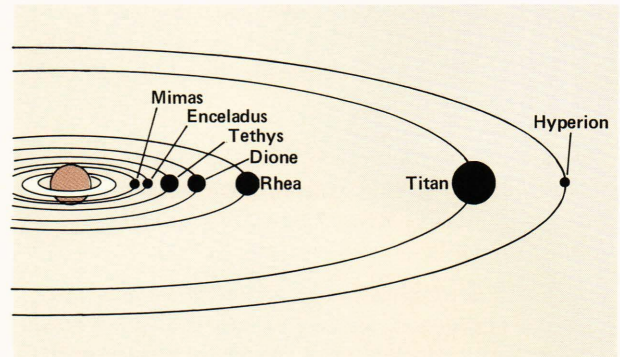


Figure 1 — A schematic representation of the Saturnian system, showing the seven major inner satellites of Saturn. Titan, the largest Saturnian satellite, is about $20 R_S$ from the planet. Water ice is believed to form the outermost layer of most satellites.

ments have revealed the rings to be an extensive and complex system of particulate matter, extending much farther out than is visible from ground-based telescopes or observed by Pioneer 11 instruments. They extend to distances perhaps as far as $8 R_S$ (R_S , the Saturn radius, is 60,330 kilometers).

The inferred average shape of the Saturnian magnetosphere is shown in Fig. 2, together with the trajectories of the two Voyager spacecraft through the system. The cutaway section shows that, on the average, the orbit of Titan is generally inside the magnetosphere, although at times Titan finds itself in the magnetosheath or even in the solar wind.² Both Voyager spacecraft approached the magnetosphere from the direction of the sun (local noon), with Voyager 1 encountering Titan on the inbound leg, dipping under the equatorial plane of Saturn, and then crossing into the northern hemisphere and leaving in the general antisolar direction. Voyager 2, on the other hand, came in above the Saturnian equatorial plane, crossed into the southern hemisphere, and left the

*A GLOSSARY of technical terms appears on page 186.

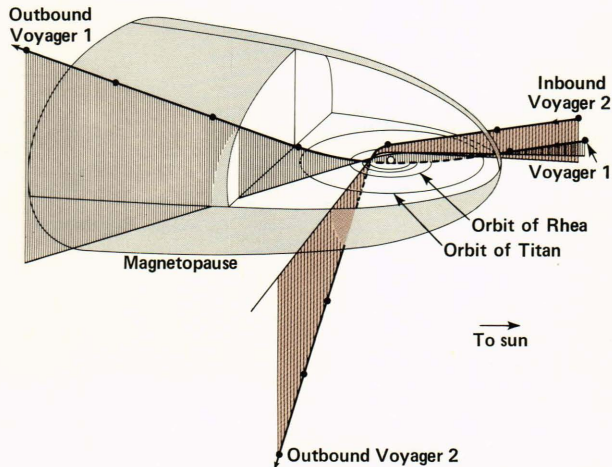


Figure 2 — Trajectories of the two Voyager spacecraft shown in the framework of an average-size magnetosphere of Saturn. On the average, the orbit of Titan lies inside the magnetopause on the sunward side.

magnetosphere in the general vicinity of local morning on its way to an encounter with Uranus in 1986. Voyager 1 approached the planet to within 126,000 kilometers above Saturn's cloud tops, while Voyager 2 came closer at a distance of 100,800 kilometers. Closest approach occurred at a south latitude of about 37° in the case of Voyager 1, but just north of the equatorial plane (8°) for Voyager 2.

ENERGETIC PARTICLE MEASUREMENTS

Among the most important questions about Saturn prior to the spacecraft encounters was whether Saturn possessed a magnetic field and trapped radiation, i.e., the equivalent of Van Allen Belts. These questions were answered in the affirmative following the Pioneer encounter in September 1979. The full extent of the magnetosphere of Saturn and its trapped particles is depicted in Fig. 3, which shows observations obtained by the APL Low Energy Charged Particle (LECP) experiment on the Voyager 2 spacecraft. The top panel shows the intensity profile of low (22 kiloelectronvolt) and intermediate (250 kiloelectronvolt) energy electrons and of high-energy protons as the spacecraft approached and then receded from the planet. The data show the magnetosphere to be populated largely by low-energy (soft) electrons in the outer regions, while more energetic electrons appear to dominate closer in. Inside the orbits of Enceladus and Mimas there appear substantial fluxes of high-energy (≥ 80 megaelectronvolt) protons, forming the hard core of the radiation belt. These protons originate from the interaction of cosmic rays with the rings of the planet, as pointed out by the Pioneer 11 investigators.³

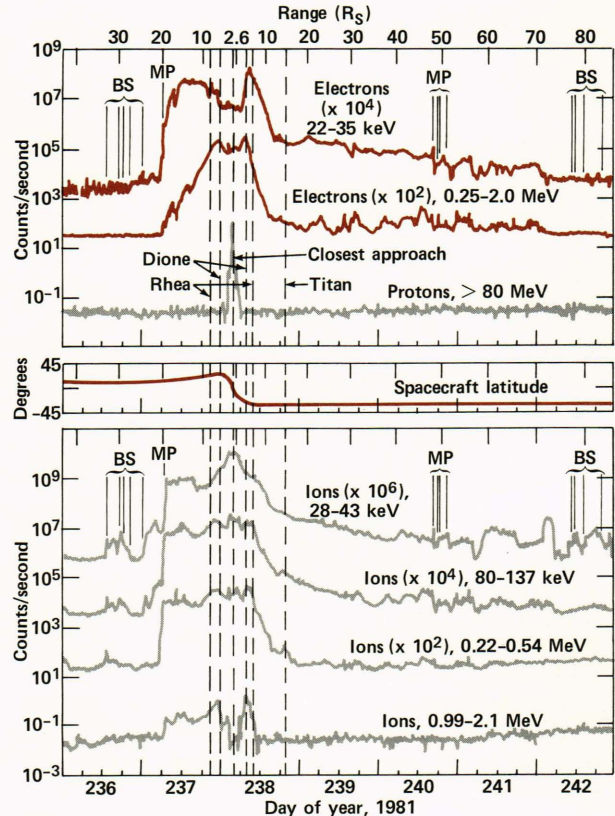


Figure 3 — Fifteen-minute averages of selected channels of the APL experiment on Voyager 2. Bow shock (BS) and magnetopause (MP) encounters are noted. Vertical dashed lines indicate crossings of outer satellite dipole L -shells.

The lower panel shows the intensity profile of energetic ions over the range from about 28 kiloelectronvolts to 2.1 megaelectronvolts. It is evident that the profile of the lowest-energy ions (top curve) is substantially different from that at the highest energy ions (bottom curve). In particular, fluxes of low-energy ions increase rapidly inside the orbit of Dione, while higher-energy ions appear to be depleted in this region. The particle intensity profile suggests that the satellites of Saturn play an important role in shaping the spatial distribution of ions within the radiation belts of the planet. A most noticeable feature of the overall energetic particle profile is the obvious asymmetry between the dayside of the planet and the early morning region, where the Voyager 2 spacecraft left the magnetosphere. The magnetopause crossing occurred at a distance of $18.5 R_S$ inbound, while the equivalent crossing outbound occurred at a distance of about $50 R_S$. It appears that the physical state of the magnetosphere of Saturn changed substantially while the spacecraft was inside.

The intensity profiles for the various energy channels in Fig. 3 suggest that the electron and ion energy

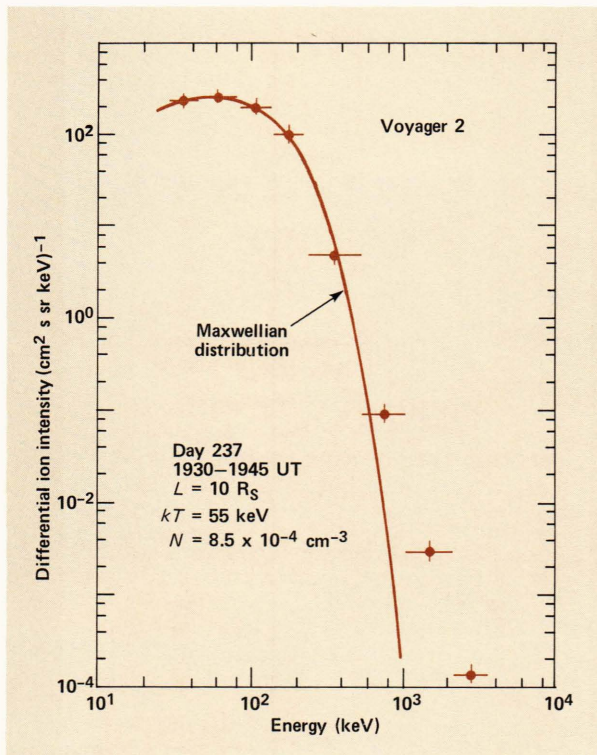


Figure 4 — Observed differential energy spectrum at the indicated radial distance, and a fit by a Maxwellian distribution (solid line) for the lower-energy channels. Note that the transition from thermal to nonthermal spectrum occurs at an ion energy of about 500 kiloelectronvolts. This is the hottest plasma ever measured in the solar system, with the characteristic temperature, kT , about 55 kiloelectronvolts.

spectra undergo considerable change as a function of distance from the planet. An example of a typical ion spectrum in the outer part of the magnetosphere is shown in Fig. 4. The spectrum seems to be described well by a Maxwellian distribution at the lowest energies of the form $j(E) = KE \exp(-E/kT)$, while at higher energies it is described well by a spectrum of the form $E^{-\text{const}}$. (E is ion kinetic energy and K is a constant). A most surprising aspect of ion spectra in the magnetosphere is that the Maxwellian temperature kT can range up to 55 kiloelectronvolts, that is, 6×10^8 K, the highest temperature recorded in the solar system.⁴

The systematic variation of kT (as a function of the crossing distance L of a dipole magnetic field line at the Saturnian equator) is shown in Fig. 5. It is seen that temperatures during the inbound part of the trajectory are generally higher than during the outbound part. Further, there appears to be a temperature maximum that is close to the orbit of Rhea on the inbound trajectory, while it is between the orbits of Rhea and Dione on the outbound trajectory. Ion intensities inside the orbit of Rhea (upper panels) are essentially the same inbound and outbound. Examination of the Voyager 1 data reveals a similar but less pronounced dependence, with peak kT about 32 kiloelectronvolts and a maximum in kT confined be-

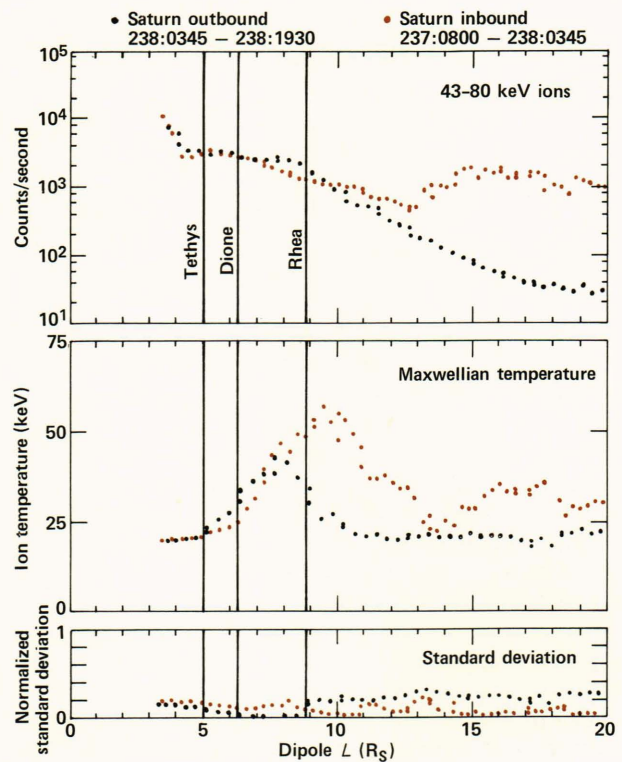


Figure 5 — The ion temperature, derived from fits similar to that shown in Fig. 4, as a function of radial distance from the planet expressed in terms of the magnetic dipole L -shell parameter. The top panel shows the characteristic intensity profile for one of the energy channels used in the fit; the bottom panel indicates the normalized goodness of fit to the Maxwellian distribution.

tween the orbits of Rhea and Tethys, both inbound and outbound.

A schematic representation of the high-temperature region observed by the Voyager 2 spacecraft is shown in Fig. 6. The asymmetry between the inbound and outbound trajectories is indicated, as is the expectation that the density of the hot plasma increases as one approaches the planetary equator. The actual observations of Voyager 2 occurred in the northern (inbound) and southern (outbound) hemispheres rather than at the planetary equator.

A measurement that can help potentially in understanding the presence of the hot plasma is the composition of the energetic particle population. However, the LECF detector cannot distinguish between energetic ions according to atomic mass at the energy range where most of the hot plasma has been measured, although it can make composition measurements at high (≥ 200 kiloelectronvolts per nucleon) energies. The composition measurements at high energies can then be extrapolated to lower energies, where most of the hot plasma resides.

Figure 7 shows a mass histogram of ions observed during the Voyager 2 encounter. The histogram on the left (Fig. 7a) shows the unambiguous presence of molecular hydrogen ions (H_2^+ , H_3^+), as well as helium ions. Krimigis *et al.*⁴ have interpreted the

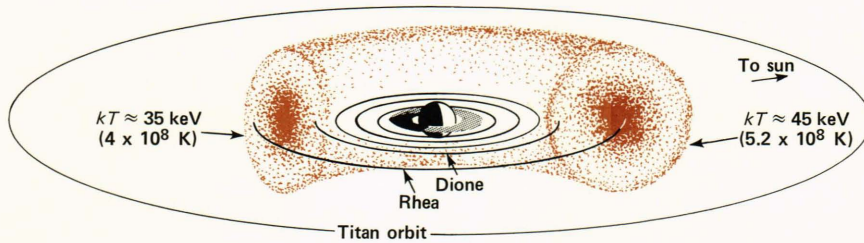


Figure 6 — A schematic view of the hot plasma torus deduced on the basis of the preceding figure. Note the day/night asymmetry. The indicated temperatures on the dayside and morningside represent the full width at half-maximum temperature deduced from the radial distribution in Fig. 5.

presence of molecular hydrogen ions as an unambiguous indicator of the presence of ionospheric plasma in the magnetosphere,⁵ because H_3^+ is expected to be present as a stable constituent of the ionosphere of Saturn. The presence of helium ions, abundant in the solar wind, indicates that solar wind plasma is also a source of energetic particles in the magnetosphere.

Figure 7b is a mass histogram of heavier ions. The solid bars correspond to observations within the magnetosphere of Saturn, while the colored line shows data obtained in the interplanetary medium representing particles of solar origin. Although the statistics are relatively poor, there appear to be two major peaks concentrated in the expected location of carbon and oxygen for both magnetospheric and solar particles. The result suggests that the solar wind is a likely source of energetic carbon particles in the magnetosphere. However, the interpretation of the oxygen peak is more difficult. Oxygen is known to be present in the solar wind and would be expected to be a constituent of the magnetospheric population; oxygen, however, is also a likely product of dissociation of water ice from the surfaces of the satellites and rings. Additional analysis is needed before the relative contributions of these two sources of oxygen to the magnetosphere of Saturn can be assessed.

PLASMAS, MAGNETIC FIELD, AND WAVES

In addition to the large fluxes of energetic particles, the magnetosphere of Saturn is populated by a low-energy plasma consisting of ions and electrons, first observed by the Pioneer 11 spacecraft.⁶ Figure 8a shows the electron density profile for this plasma as observed by the Voyager 2 spacecraft.² Peak intensities are observed in the vicinity of the satellites Rhea through Enceladus, i.e., in the same region where the hot plasma torus consisting of energetic particles was observed. The density of the low-energy plasma is about one ion per cubic centimeter, i.e., a thousand times higher than that of the hot plasma. The Pioneer investigators found that the dominant component of this relatively "cold" plasma is oxygen, a result corroborated by the Voyager investigators. The likely origin is thought to be dissociation of water through sputtering of ice caused by energetic ions incident on the surfaces of the icy satellites.⁷ Figure 8b shows the estimated vertical extent of the Saturn plasma sheet; it combines the data obtained by Voyager 2, Voyager 1, and Pioneer 11. The darker

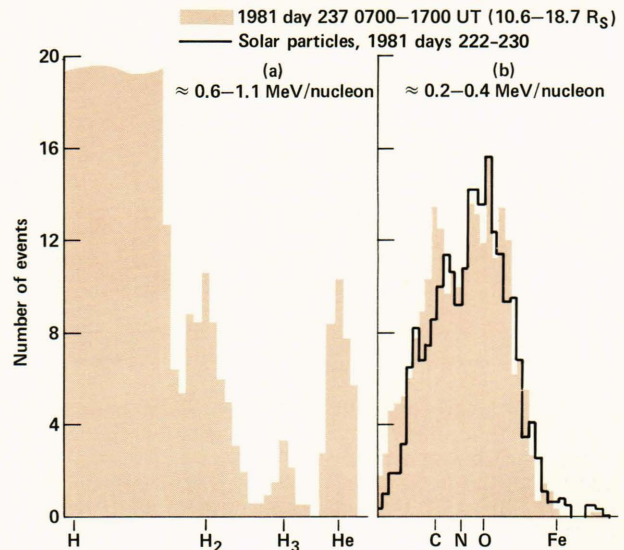


Figure 7 — A mass histogram of energetic ions observed with the LECP experiment during the early part of the inbound trajectory on Voyager 2. (a) A histogram of the light ions; the hydrogen peak on the left is large and has been cut off. (b) A histogram of the heavier ions, together with data obtained prior to spacecraft entry into the magnetosphere, for comparison.

region refers to a plasma containing only oxygen ions and electrons and the lighter region to one containing protons and electrons. Much remains to be done in understanding fully the plasma configuration in the magnetosphere of Saturn.

The analysis of the magnetic field, on the other hand, is at an advanced stage. Magnetometers on both the Voyager and the Pioneer spacecraft have done a rather detailed mapping of the magnetic field environment of the planet.⁸⁻¹⁰ A most surprising finding is that the magnetic dipole moment of Saturn is inclined no more than 1° from the rotational axis of the planet. This is in contrast to the cases of Jupiter, Earth, and Mercury, where the magnetic moment is tilted with respect to the rotational axis of the planets by 11° , 10° , and 12° , respectively. The planetary magnetic field has a magnetic dipole moment of 0.21 gauss-R_S^3 , substantially less than that expected on the basis of various scaling laws.¹¹ The center of the dipole is thought to be within $0.02 R_S$ of the geometrical center of Saturn.

The magnetic field differs from a perfect dipole as a result of the influence of the ring current, repre-

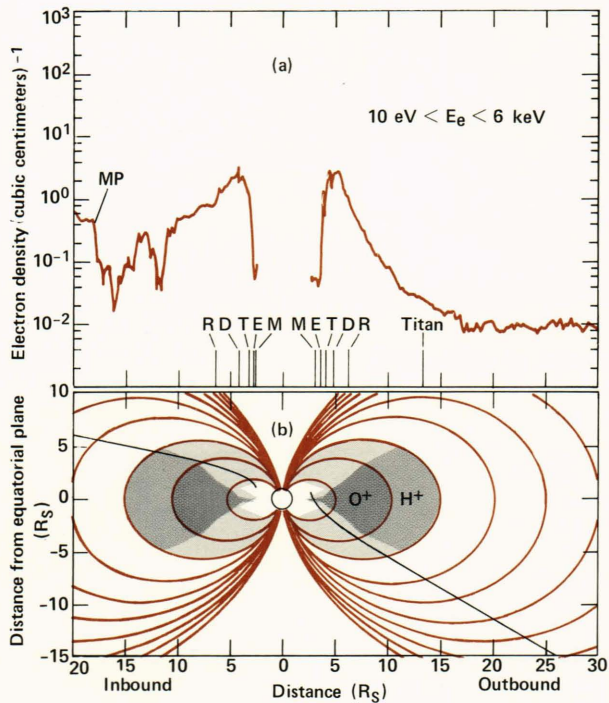


Figure 8 — (a) The electron density profile as observed by the plasma instrument on Voyager 2 as a function of the equatorial crossing distance of a dipole field line. Note the density peak in the region of the orbits of Rhea (R), Dione (D), and Tethys (T), both inbound and outbound, and the basic day/night asymmetry of the magnetosphere. (b) The meridional extent of the plasma sheet indicating both the regions where hydrogen ions dominate (light shading) and where oxygen ions dominate (dark shading).²

sented by the observed plasma trapped within the magnetosphere of Saturn. A first model of the effects of the ring current is shown in Fig. 9.¹² The figure shows a meridian plane projection of magnetic field lines for a dipole field model (dashed lines) and a model that contains a distributed ring current outlined by the shaded region within the figure (solid lines). It is evident that the effect of the ring current is to distend the field lines of the nominal dipole at distances as close as the orbit of Dione. This particular model, based on the observations from the Voyager 1 spacecraft, does not appear to fit the Voyager 2 data very well,¹⁰ suggesting that there were significant changes in the magnetosphere of Saturn between the Voyager 1 and Voyager 2 encounters.

Associated with the plasmas and energetic particles in the magnetosphere of Saturn (as well as at the magnetospheres of other planets) is a large variety of plasma wave emissions ranging in frequency from a few hertz (Hz) to several kilohertz (kHz). These waves are trapped within the magnetosphere of the planet and can only be observed with *in situ* investigations. Such waves exhibit characteristic signatures at the crossing of the planetary bow shock and magnetopause, as well as inside the magnetosphere. An example of the plasma wave observations from Voyager 2 near closest approach is given in Fig. 10.¹³ The

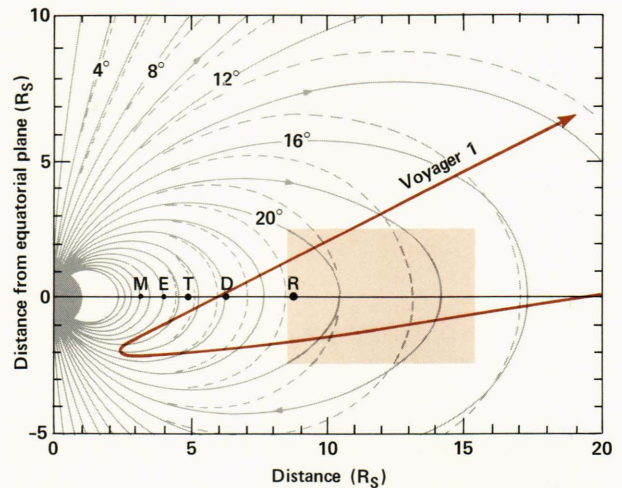


Figure 9 — Magnetic field model of Saturn's dipole based on the Voyager 1 data. The magnetic and rotational axes of Saturn are aligned to within 1°; the dashed lines indicate field lines for a pure dipole, while the solid lines indicate distended field lines due to the presence of the ring current, as indicated by the shaded region extending from about 8.5 to 15.3 R_S (adapted from Connerney *et al.*).¹² Note that the sense of Saturn's magnetic field is opposite that of Earth, i.e., field lines are leaving the North Pole.

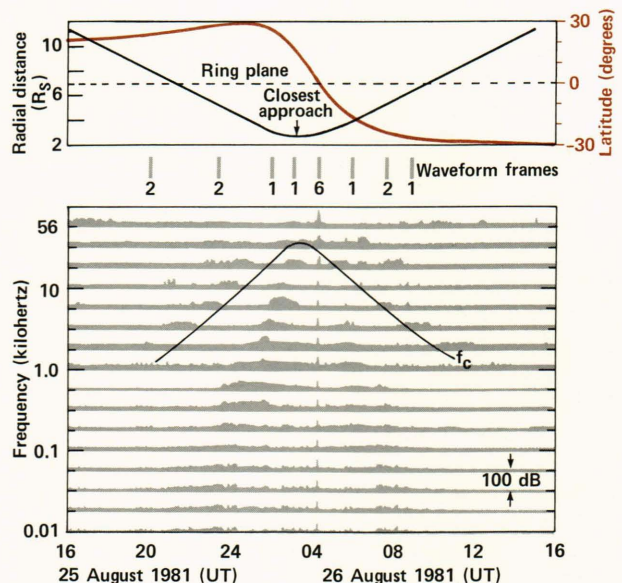


Figure 10 — Observations of plasma wave activity during the Voyager 2 encounter (adapted from Gurnett *et al.*).¹⁴ The electron cyclotron frequency, f_c , is noted by the solid line. Features of this plot are explained in the text.

figure shows intensities of the electric field component of plasma waves in a 16-channel analyzer ranging in frequency from 10 Hz (the lowest channel) to 56 kHz (the highest channel). The solid line indicates the electron cyclotron frequency, f_c , which is determined by the magnitude of the magnetic field. Other plasma wave parameters include the electron plasma frequency, f_p , which is directly related to the local plasma density and in some cases can be used to deduce the plasma density directly.¹⁴ Typically, it is rel-

actively easy to identify the combination of f_c and f_p , which is the upper hybrid resonance (UHR) and is related to f_c and f_p via the relation $f_{\text{UHR}}^2 = f_c^2 + f_p^2$. Some UHR emissions can be identified in the figure, for example, the one at 10 kHz at 2040 to 2120 UT on 25 August. Thus, it is possible with the knowledge of f_c (determined from the magnetic field magnitude) to identify the values of f_p and, consequently, the value of the local plasma density.

We note from Fig. 10 that the low-frequency emission increased substantially as the spacecraft approached the planet. Also notable is an intensity peak at 0418 UT on 26 August that is independent of frequency and occurs at the time of crossing of the Saturnian equatorial plane. Scarf *et al.* attribute this peak to hits on the spacecraft by ring particles.¹³ In addition to these broadband emissions, a number of discrete emissions have been detected during both the Voyager 1 and Voyager 2 encounters that can be associated with specific local plasma phenomena in the magnetosphere of Saturn.^{13,15}

SATURNIAN RADIO EMISSION

While low-frequency plasma waves cannot escape from the magnetosphere, radio waves generated in the vicinity of the planet can propagate relatively freely through the magnetosphere to the interplanetary medium. The first evidence of radio waves from Saturn were obtained by the Voyager 1 spacecraft well over a year prior to its encounter with Saturn. Kaiser *et al.*¹⁶ were able to establish, through a power spectrum analysis, that the source of the waves was rotating with a period of 10 h 39 m 24 s, which was substantially different from the planetary rotation period of 10 h 15 m established on the basis of optical observations from earth. Subsequent analysis of a larger body of data¹⁷ has shown the mean rotation period to be 10 h 39 m 22 s.

The frequency spectrum of the Saturnian radiation, called Saturnian kilometric radiation (SKR) because of its kilometer-long wavelength, is shown in Fig. 11.¹⁷ The peak flux occurs in the range of 100 to 200 kHz, with an apparent cutoff at 1000 kHz at the high end and about 20 kHz at the low end. As noted earlier, the emission continues below 20 kHz, but it is generally trapped within the magnetosphere of the planet. In this figure, the right-hand and left-hand polarized emissions have been combined, and the two curves represent the average flux density (lower curve) and peak flux density or 97th percentile flux (upper curve). Integration of the average curve in this figure yields an equivalent power per unit area at one astronomical unit (1.5×10^8 kilometers) of 5.3×10^{-15} watts per square meter. The corresponding isotropic equivalent average power of the Saturnian radio source is about 1.5×10^9 watts, which is approximately 0.4% of the Jovian radio emission below 40 MHz but about five times that of the Jovian kilometric emission below 300 kHz.¹⁷

The fact that the SKR is modulated with the planetary rotation period would suggest that there is a

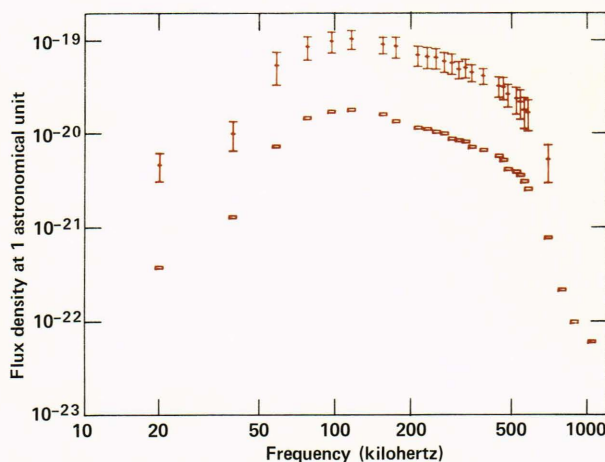


Figure 11 — Distribution of the average flux density (lower curve) and of “peak” or 97th percentile flux density (upper curve). Flux densities are in watts per square meter per hertz (adapted from Carr *et al.*¹⁷).

source region that seems to be rotating with the planet. The easiest explanation would have been that the modulation results from the tilt of the planetary magnetic field. As we have seen, however, the Saturnian magnetic field is tilted by less than 1° , so it is difficult to see how that small tilt could produce such large modulation. The possibility of the existence of a magnetic anomaly in the Saturnian magnetic field has been examined in detail,¹⁰ but so far the results have been negative. However, the combined observations from the two spacecraft have enabled Kaiser and Desch¹⁸ to pinpoint the source of SKR to a region in the northern hemisphere of the planet around local noon. This is shown in Fig. 12, taken from Kaiser and Desch,¹⁸ who have identified the source region of right-handed polarized emission as a spot at about 75° latitude in the northern hemisphere close to the noon meridian. Left-handed emission is from the southern hemisphere. Thus, Saturnian kilometric radiation comes from specific regions rotating with Saturn that only turn on and emit radio waves when they cross the general vicinity of local noon. In this sense, SKR does not resemble a rotating searchlight, but rather a searchlight that is generally off and only turns on in a particular direction. It should be noted that the Saturnian kilometric radiation is also modulated by the satellite Dione,¹⁵ in an as yet undetermined manner.

In addition to SKR, another type of radio emission was observed by the Planetary Radio Astronomy investigators on both Voyager 1 and Voyager 2 spacecraft. The nature of this phenomenon, named Saturn electrostatic discharge (SED), is shown in Fig. 13. The SED's are the sharp spikes superimposed on the overall SKR emission as the Voyager 1 spacecraft approached the planet and then receded.¹⁹ These emissions appear over the entire frequency range of the instrument, from 20 kHz to 40 MHz, and their intensity increased as the spacecraft approached the planet's rings. The investigators have concluded that

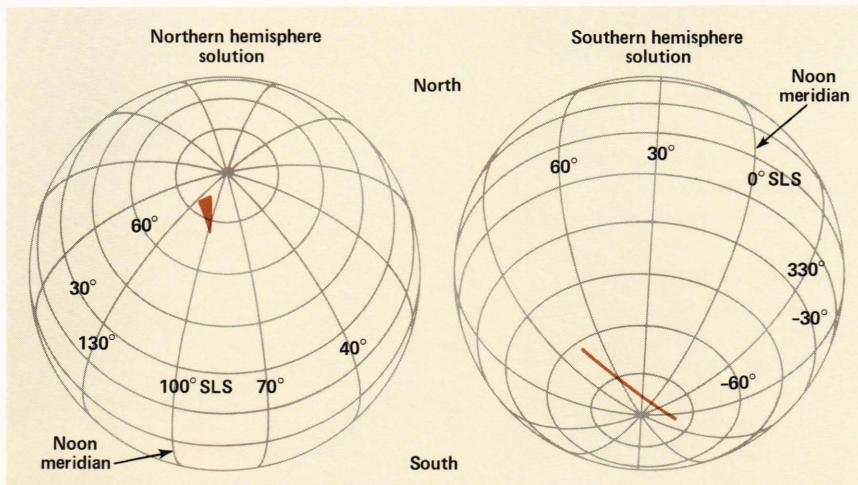


Figure 12 — Best estimates of the location of Saturnian kilometric radiation source as deduced by Kaiser and Desch.¹⁸ Right-handed polarized emission comes from a small area in the northern hemisphere, while left-handed polarized emission maps to a narrow band at high latitudes in the southern hemisphere.

GLOSSARY

Electron cyclotron frequency. f_c , equals $28 B$, where B , the magnetic field strength, is given in nanoteslas. (One nT equals 10^{-5} gauss.)

Electron plasma frequency. f_p , equals $9\sqrt{N}$, where the plasma frequency is in hertz and N is the number of ions per cubic centimeter.

Flux density. The intensity of radio emission in terms of power per unit area per unit frequency interval.

Ionospheric plasma. The electrons and ions that form the ionosphere of a planet.

L-shell parameter. A parameter designating a surface of revolution generated by a magnetic field line rotated about the axis of the magnetic moment vector in a dipole-like magnetic field. Its numerical value equals the distance (in planetary radii) at which the magnetic field line crosses the equatorial plane.

Lobe field line. A field line in the antisolar direction of a magnetosphere that maps to relatively high ($\geq 60^\circ$) latitudes and does not reach the other hemisphere; it interconnects with field lines of the interplanetary magnetic field.

Magnetic dipole moment. The strength of the magnetic dipole of a planet, expressed in $\text{gauss} \cdot R_p^3$, where R_p is the planet's radius.

Magnetopause. A surface separating the region of space controlled by the solar wind from that controlled by the planetary magnetic field.

Magnetosheath. The region, just ahead of the magnetopause, in which the solar wind has become thermalized.

Magnetosphere. That region of space around a planet that is controlled by the planetary magnetic field.

Maxwellian temperature. The temperature of a gas that is described by the Maxwell distribution of velocities.

Meridian plane projection. Projection onto a plane defined by a

meridian and the planet's rotation axis. In the case of the spacecraft's trajectory, both the inbound and outbound parts are projected onto the same plane.

Particulate matter. Neutral molecules, neutral atoms, and dust particles.

Plasma density (N). The number of charged ions or electrons per unit volume.

Plasma wave emission. Wave emission associated with the local plasma.

Ring current. Ions and/or electrons undergoing drift motions about the planet.

Solar wind. Ionized gas emitted by the sun and propagating radially outward at speeds ranging from about 300 to more than 1000 kilometers per second. It is an extension of the sun's corona.

Thermal spectrum. A spectrum described by a Maxwellian energy distribution.

Torus. A doughnut-shaped object.

$j(E)$. The number of particles per unit area, solid angle, time, and energy interval.

LECP. The Low Energy Charged Particle experiment on the Voyager 1 and Voyager 2 spacecraft.

R_S . Saturn radius (60,330 kilometers at the equator).

SED. Saturn electrostatic discharge.

SKR. Saturn kilometric radiation.

SLS. Saturn Longitude System (Epoch 1980.0), i.e., at 0 hr UT on January 1, 1980 at which time the prime meridian of Saturn (0° SLS) is defined to be coincident with Saturn's vernal equinox.

UHR. Upper hybrid resonance.

UT. Universal time.

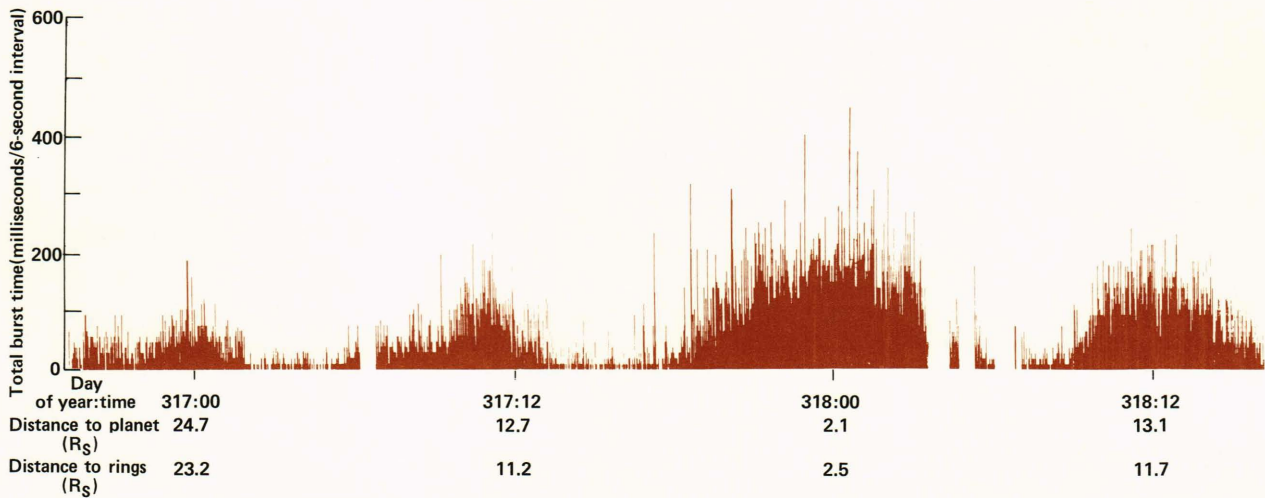


Figure 13 — Occurrence of Saturn electrostatic discharges (SED) as a function of time and distance from closest approach during the Voyager 1 encounter (adapted from Warwick *et al.*¹⁹).

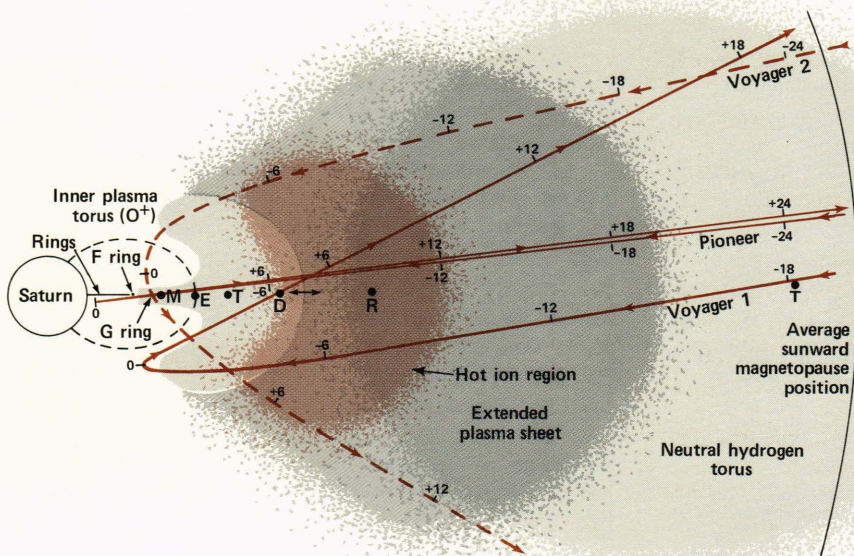


Figure 14 — A schematic summary in meridional cross section of the various regions in Saturn's magnetosphere (adapted from Stone and Miner).²³ In addition to various plasma regions described in the text, Titan's neutral hydrogen torus is shown. The locations of the orbits of the major satellites are shown by filled circles and are labeled by the satellite's initial. Also shown in meridional projections are the time-tagged (hours from Saturn closest approach) trajectories of Pioneer 11, Voyager 1, and Voyager 2. It is evident from the figure that trajectories of the three spacecraft were complementary and performed measurements through large regions of the magnetosphere of Saturn.

they are caused by electrostatic discharges within the rings, at a period of about 10 h 10 m. The source of SED appears to be in the ring system at about 1.81 R_S from the center of the planet and could be related to the spokes observed in the rings by the imaging investigation.²⁰ Further analysis, in combination with data from other experiments, will undoubtedly illuminate this most surprising aspect of Saturnian radio emissions.

SUMMARY AND DISCUSSION

Space does not permit a more detailed discussion of several other related observations that are relevant to the Saturnian environment. One of these, for example, is the presence of a neutral hydrogen torus

that extends from beyond the orbit of Titan to inside the orbit of Rhea and has a density of about 10 atoms per cubic centimeter.²¹ The source of this hydrogen is undoubtedly the atmosphere of Titan; energetic ions in the magnetosphere charge exchange with the neutral hydrogen and escape as fast neutrals from the magnetosphere through that process.²²

Figure 14 summarizes some of the major results obtained by the encounters of the Pioneer and Voyager spacecraft in the environment of Saturn.²³ The figure shows a schematic cross section of Saturn's magnetosphere. The hydrogen torus dominates the magnetosphere although, being neutral, it does not participate directly in magnetosphere dynamics. The extended plasma sheet is indicated, as are the hot ion

region observed by the LECP experiment and the inner plasma torus thought to contain primarily oxygen ions. The average sunward location of the magnetopause is generally beyond the orbit of Titan and is determined by the pressure balance between the solar wind and the planetary magnetic field. In this sense, the magnetosphere of Saturn is very much different from that of Jupiter, where the location of the sunward magnetopause is determined by the pressure balance between the hot Jovian plasma and the solar wind, rather than by the planetary magnetic field.

The magnetosphere of Saturn is different from those of Jupiter and Earth in other respects as well. During the traversal of the Voyager 1 spacecraft through the region of the Saturnian magnetic tail, it was noted that energetic electrons were observed all the way to the magnetopause,²⁴ indicating that field lines in the tail lobe of the magnetosphere of Saturn are closed. This is in contrast to both Earth and Jupiter, where lobe field lines are generally open and devoid of either plasma or energetic particles. The absence of continuum radiation in that region of Saturn's magnetosphere,¹⁵ in contrast to the presence of such radiation at Earth and Jupiter, is another indication that the magnetosphere of Saturn may be closed, the only such magnetosphere in the solar system (with the possible exceptions of Uranus and Neptune, which have not yet been explored).

The detailed analysis of the Voyager 1 and Voyager 2 encounters with Saturn is presently under way and will continue for at least the next two years. Undoubtedly, when the results from the individual experiments are combined, new insights will result into the general characteristics and dynamics of the magnetosphere itself and its interaction with the rings, planetary satellites, and ionosphere of the planet.

REFERENCES

- ¹*Science* **207**, 400-449 (1980).
- ²H. S. Bridge *et al.*, "Plasma Observations near Saturn: Initial Results from Voyager 2," *Science* **215**, 563-570 (1982).
- ³W. Fillius and C. McIlwain, "Very Energetic Protons in Saturn's Radiation Belt," *J. Geophys. Res.* **85**, 5803-5811 (1980).

- ⁴S. M. Krimigis *et al.*, "Low-Energy Hot Plasma and Particles in Saturn's Magnetosphere," *Science* **215**, 571-577 (1982).
- ⁵D. C. Hamilton *et al.*, "Detection of Energetic Hydrogen Molecules in Jupiter's Magnetosphere by Voyager 2: Evidence for an Ionospheric Plasma Source," *Geophys. Res. Lett.* **7**, 813-816 (1980).
- ⁶L. A. Frank *et al.*, "Plasmas in Saturn's Magnetosphere," *J. Geophys. Res.* **85**, 5695-5708 (1980).
- ⁷A. F. Cheng, L. J. Lanzerotti, and V. Pirronello, "Charged Particle Sputtering of Ice Surfaces in Saturn's Magnetosphere," *J. Geophys. Res.* **87**, 4567-4570 (1982).
- ⁸E. J. Smith *et al.*, "Saturn's Magnetic Field and Magnetosphere," *Science* **207**, 407-410 (1980).
- ⁹N. F. Ness *et al.*, "Magnetic Field Studies by Voyager 1: Preliminary Results at Saturn," *Science* **212**, 211-217 (1981).
- ¹⁰N. F. Ness *et al.*, "Magnetic Field Studies by Voyager 2: Preliminary Results at Saturn," *Science* **215**, 558-563 (1982).
- ¹¹C. T. Russell, "Re-evaluating Bode's Law of Planetary Magnetism," *Nature* **272**, 147 (1978).
- ¹²J. E. P. Connerney, M. H. Acuna, and N. F. Ness, "Saturn's Ring Current and Inner Magnetosphere," *Nature* **292**, 724-726 (1981).
- ¹³F. L. Scarf *et al.*, "Voyager 2 Plasma Wave Observations at Saturn," *Science* **215**, 587-594 (1982).
- ¹⁴D. A. Gurnett *et al.*, "Determination of Jupiter's Electron Density Profile from Plasma Wave Observations," *J. Geophys. Res.* **86**, 8199-8212 (1981).
- ¹⁵D. A. Gurnett, W. S. Kurth, and F. L. Scarf, "Plasma Waves Near Saturn: Initial Results from Voyager 1," *Science* **212**, 235-239 (1981).
- ¹⁶M. L. Kaiser *et al.*, "Voyager Detection of Nonthermal Radio Emission from Saturn," *Science* **209**, 1238-1240 (1980).
- ¹⁷T. D. Carr, J. J. Schauble, and C. C. Schauble, "Pre-encounter Distributions of Saturn's Low Frequency Radio Emission," *Nature* **292**, 745-747 (1981).
- ¹⁸M. L. Kaiser and M. D. Desch, "Saturnian Kilometric Radiation: Source Locations," *J. Geophys. Res.*, in press (1982).
- ¹⁹J. W. Warwick *et al.*, "Planetary Radio Astronomy Observations from Voyager 1 Near Saturn," *Science* **212**, 239-243 (1981).
- ²⁰J. W. Warwick *et al.*, "Planetary Radio Astronomy Observations from Voyager 2 Near Saturn," *Science* **215**, 582-587 (1982).
- ²¹B. R. Sandel *et al.*, "Extreme Ultraviolet Observations from the Voyager 2 Encounter with Saturn," *Science* **215**, 548-553 (1982).
- ²²E. Kirsch *et al.*, "X-ray and Energetic Neutral Particle Emission from Saturn's Magnetosphere," *Nature* **292**, 718-721 (1981).
- ²³E. C. Stone and E. D. Miner, "Voyager 2 Encounter with the Saturnian System," *Science* **215**, 499-504 (1982).
- ²⁴S. M. Krimigis *et al.*, "Low-Energy Charged Particles in Saturn's Magnetosphere: Results from Voyager 1," *Science* **212**, 225-231 (1981).

ACKNOWLEDGMENTS — I would like to thank the LECP co-investigators for their contributions to the experiment and analysis of the results described in this paper. Dr. J. F. Carbary has contributed much work in generating some of the figures. The LECP program was supported at APL by NASA under Task I of Contract N00024-78-C-5384 between The Johns Hopkins University and the Department of the Navy.